PAPER

CrossMark
click for updates

{Co₅^II/III} horseshoe and {Ni₄^II} lacunary cubane coordination clusters: the isobutyrate/N-butyldiethanolamine reaction system†

Sebastian Schmitz,[a] Kirill Yu. Monakhov,[a] Jan van Leusen,[a] Natalya V. Izarova,[b] Volkmar Heß[ab] and Paul Kögerler*[ab]

The polynuclear coordination compounds [Co₃^II Co₂^III(Hbda)₂(bda)₂(ib)₆]·2MeCN (**1**) and [Ni₄^II(Hbda)₃ (ib)₅(MeCN)] (**2**) (H₂bda = *N*-butyldiethanolamine, ib = isobutyrate) are prepared under aerobic conditions using an identical synthetic protocol that solely differs in the employed transition metal (Co^II *vs.* Ni^II). Whereas compound **1** displays a mixed-valent, pentanuclear, horseshoe-shaped structure with alternating Co(ɪɪ) and Co(ɪɪɪ) ions, compound **2** presents a tetrahedrally-shaped Ni(ɪɪ) structural motif where four nickel centers are bridged by three O atoms to afford a lacunary Ni₄O₃ cubane, a motif hitherto only observed as a substructure of higher-nuclearity coordination clusters and polyoxometalates. Both compounds are thermally surprisingly stable (>130 °C). **1** exhibits weak antiferromagnetic exchange interactions; **2** shows a ferromagnetic coupled triangle of three Ni centers interacting antiferromagnetically with a single Ni apex.

Introduction

Polynuclear transition metal coordination compounds are an attractive, large playground for comparative experimental and computational studies[1] of their bulk-to-surface structure–magnetism relations, in particular in the area of molecular conductivity and spintronics[2] and quantum computing.[3] When we aim to explore the charge transport characteristics of discrete coordination complexes (where studies in the literature thus far predominantly focus on single-molecule magnets[4]) *via* magnetic (*e.g.* X-ray magnetic circular dichroism) or scanning probe microscopy experiments,[5] important molecular characteristics for their deposition on a substrate are: low-nuclearity, charge neutrality, moderate solubility and structural stability in organic solvents, thermal stability and sublimability. Furthermore, even paramagnetic coordination clusters with no magnetic anisotropy-induced slow magnetization relaxation or hysteresis (as opposed to SMMs) generate considerable interest if they can be deposited as intact, single molecules, as they can undergo substantial changes in their molecular magnetic anisotropy upon redox processes (see, *e.g.*, reduction of Mn^III to

Mn^II in the mixed-valent {Mn₁₂^III Mn₇^II} coordination cluster on Au(111)[6]) at the molecule–surface interface or by external electromagnetic fields.

We here report a simple reaction system that results in thermally stable, low-nuclearity, charge-neutral coordination clusters [Co₃^II Co₂^III(Hbda)₂(bda)₂(ib)₆]·2MeCN (**1**) or [Ni₄^II(Hbda)₃ (ib)₅(MeCN)] (**2**) which fall into the archetypal horseshoe-[7] and cubane-[8] type structure families, from which numerous chemically[9] and magnetically functionalized derivatives can then be generated. **1** and **2** were obtained under aerobic conditions in the reactions of M(ib)₂ (M = Co and Ni) and *N*-butyldiethanolamine in acetonitrile (MeCN) and were characterized by elemental analysis, IR spectroscopy, electrospray ionization mass spectrometry (ESI-MS), thermogravimetric analysis (TGA), X-ray photoelectron spectroscopy (XPS) and single-crystal X-ray diffraction, and by ac and dc susceptibility measurements that were reproduced using CONDON 2.0.[10]

Results and discussion

Synthetic procedures and stability

The isobutyrate precursors[11] M(ib)₂ (see ESI† for IR spectra) were freshly prepared by heating M(OOCMe)₂·4H₂O (M = Co, Ni) in an excess of isobutyric acid at 150 °C until all organic acid was evaporated.[12] The facile reactions of the thus-obtained M(ib)₂ powders with H₂bda in a 1 : 1 ratio in MeCN under reflux conditions (Scheme 1) in the presence of air oxygen afforded the dark-green pentanuclear mixed-valent {Co₃^II Co₂^III} complex (**1**) and the light-green homovalent tetranuclear {Ni₄^II} complex (**2**), which were isolated in yields of 49% and 22%, respectively. TGA of

ᵃInstitut für Anorganische Chemie, RWTH Aachen University, Landoltweg 1, 52074 Aachen, Germany. E-mail: paul.koegerler@ac.rwth-aachen.de

ᵇJülich-Aachen Research Alliance (JARA-FIT) and Peter Grünberg Institute (PGI-6), Forschungszentrum Jülich, 52425 Jülich, Germany

† Electronic supplementary information (ESI) available: Crystal data and structure refinement details, IR, ESI-MS, TGA and XPS data. CCDC 1487791 and 1487792. For ESI and crystallographic data in CIF or other electronic format see DOI: 10.1039/c6ra19232g
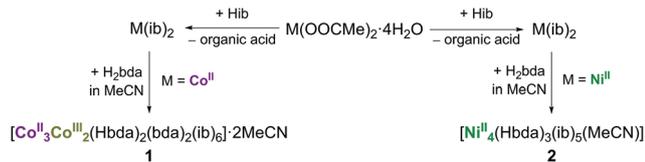
Scheme 1 Synthesis of pentanuclear compound **1** and tetranuclear compound **2**.

compound **1** confirms that the solvent-free $[Co_3^{II}Co_2^{III}(Hbda)_2(bda)_2(ib)_6]$ complex retains its integrity up to 140 °C against degradation under a nitrogen atmosphere or air (Fig. S8 and S9†). Compound **2** is thermally stable up to 130 °C (Fig. S10 and S11†).

X-ray crystal structure analysis

Complex **1** crystallizes in the triclinic space group $P\bar{1}$. Its molecular structure (Fig. 1) reveals a horseshoe-shaped metal core with Co atoms alternating in their formal oxidation states of +II and +III, established by bond valence sum analysis $[\Sigma_{bv}(Co^{II}) = 1.74–2.07$ and $\Sigma_{bv}(Co^{III}) = 2.91$ and $2.94]$, reflecting partial oxidation of Co(II) by air oxygen throughout the synthesis. XPS analysis also confirms the mixed-valent Co(II/III) formulation of compound **1** (Fig. S12†). The Co ions are ligated by four *N*-butyldiethanolamine and six isobutyrate groups. Co1, Co2, Co4 and Co5 adopt pseudo-octahedral NO_5 coordination
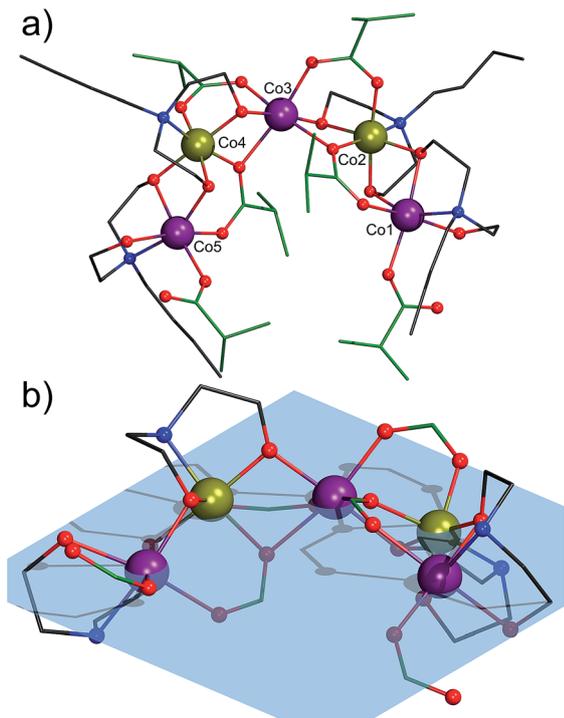

Fig. 1 (a) Molecular structure of $[Co_3^{II}Co_2^{III}(Hbda)_2(bda)_2(ib)_6]$ in **1** emphasizing the horseshoe-type structure and Co atom numbering. (b) Perspective showing the common plane (transparent blue) spanned by the five Co centers in **1**, with terminal butyl/isopropyl residues not shown. Color code: Co(II), violet; Co(III), dark yellow; C(bda), grey; C(ib), green; N, blue; O, red. Hydrogen atoms are omitted for clarity.

environments, while Co3 ion is ligated by six O atoms. All Co atoms are very close to a common plane (Fig. 1b).

Co⋯Co distances range from 2.963(1) to 3.032(1) Å. The distance between the equal $Co^{II}1$ and $Co^{II}5$ centers is 7.509(1) Å and their distance to $Co^{II}3$ ranges from 5.275(1) Å (Co1⋯Co3) to 5.257(1) Å (Co5⋯Co3). The Co1–Co2–Co3 angle is 122.99(3)°, Co3–Co4–Co5: 123.00(3)°. One monodentate μ_1-ib$^-$ ligand coordinates to each Co1 and Co5. These two ib$^-$ ligands are assumed to be deprotonated, because of their short C–O bond lengths of 1.256(7) Å (C1B1–O2B1) and 1.247(8) Å (C1B6–O2B6). The terminal monodentate ib$^-$ ligands form strong H bonds with the monoprotonated Hbda$^-$ ligands with O⋯O distances of 2.513(6)–2.526(6) Å. The μ_2-O of the Hbda$^-$ is assumed to be protonated, given the BVS values of −1.18 and −1.21 (C–O bond lengths of 1.425(7) and 1.442(10) Å) as compared to the deprotonated arms of Hbda$^-$: 1.400(7) Å and 1.404(7) Å (BVS: −2.00 and −2.03). Co1, $Co^{III}2$ and Co3 as well as Co3, $Co^{III}4$ and Co5 are bridged by a $\mu_2,\eta^1:\eta^2$ ib$^-$ ligand. In addition, Co1 and Co2 as well as Co4 and Co5 are linked by Hbda$^-$ and bda^{2-} ligands through the bridging ethanolate groups. The Co^{III} ion (Co2 and Co4) is connected with Co3 by a $\mu_2,\eta^1:\eta^1$-ib$^-$ ligand and an ethanolate group of bda^{2-}. The distance between the two Co^{III} ions is 5.783(1) Å (Co2–Co3–Co4: 145.80(3)°).

We note that in 2015 Lazzarini *et al.*[13] described a bent mixed-valent $\{Co_3^{II}Co_2^{III}\}$ complex with the Co^{II}–Co^{II}–Co^{II} angle of 138.98(1)° that was obtained in 8% yield by reacting a $[Co_2(H_2O)(piv)_4(Hpiv)_4]$ precursor (Hpiv = pivalic acid) with a Schiff-base ligand and triethylamine in MeCN. Contrary to compound **1** bearing two different types of ligands (carboxylate and aminoalcohol) and a metal core with alternating Co(II) and Co(III) centers, the pentanuclear $\{Co_3^{II}Co_2^{III}\}$ core in the reported complex consists of three inner cobalt(II) atoms and two terminal cobalt(III) atoms and is supported by six μ-carboxylate ligands, two Schiff-base ligands, two μ_3-OH groups and four terminal water molecules that complete the octahedral coordination of some Co(II) centers.

Complex **2** crystallizes in the orthorhombic space group $P2_12_12_1$. Its molecular structure consists of four octahedrally coordinated Ni^{II} ions, three partially deprotonated Hbda$^-$ ligands, three bidentate and two monodentate ib$^-$ ligands and one terminally coordinated MeCN molecule (Fig. 2). The nickel atoms form a distorted tetrahedron with the non-bonding Ni⋯Ni distances ranging from 2.9953(9) to 3.851(1) Å. The apex (Ni1) is 2.042 Å above the Ni2/Ni3/Ni4 triangle. Ni1 is surrounded by six O atoms: (i) three of these belong to the bidentate $\mu_2,\eta^1:\eta^1$-ib$^-$ ligands (Ni1–O$_{ib}$: 2.018(4)–2.046(4) Å); (ii) the other three are the μ_4-O atoms of the Hbda$^-$ ligands (Ni1–O$_{Hbda}$: 2.096(4)–2.131(4) Å). Ni2 and Ni3 reside in NO_5 environments from two μ_4-O atoms of Hbda$^-$ (Ni2-μ_{4Hbda}-O: 2.057(4)–2.091(4) Å and Ni3-μ_{4Hbda}-O: 2.063(4)–2.105(4) Å), one μ_2-O of Hbda$^-$ (Ni2–O1N2: 2.123(4), Ni3–O1N3: 2.138(3) Å), one N atom of Hbda$^-$ (Ni2–N2: 2.149(5), Ni3–N3 2.165(5) Å), and the O atoms of the bidentate (Ni2–O2B1: 2.044(4), Ni3–O2B2: 2.013(4) Å) and monodentate (Ni2–O1B5: 2.075(4), Ni3–O1B4: 2.068(4) Å) ib$^-$ ligands. The N_2O_4 environment of Ni4 is characterized by Ni4–N$_{MeCN}$: 2.122(5), Ni4–N$_{Hbda}$: 2.137(5), Ni4-μ_{4Hbda}-O: 2.054(4)–2.062(4), Ni4-μ_{2Hbda}-O: 2.103(4) and Ni4–O$_{ib}$: 2.014(4) Å.

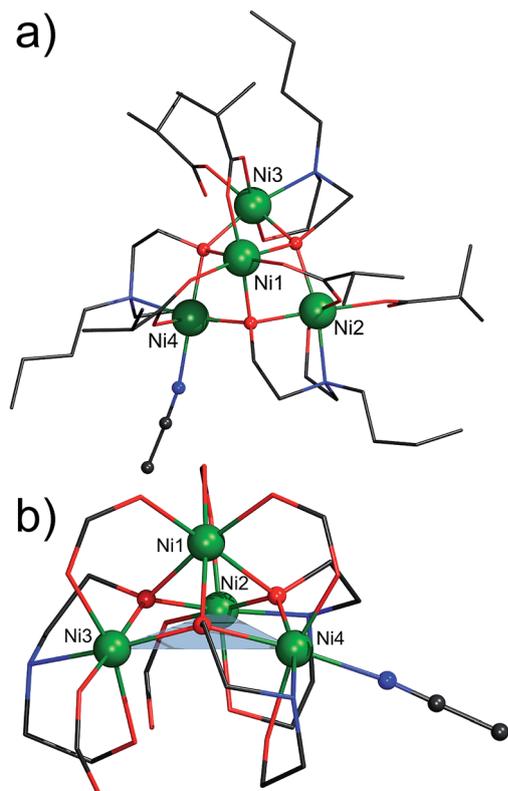**Fig. 2** (a) Molecular structure of $[Ni_4(Hbda)_3(ib)_5(MeCN)]$ in **2** with Ni atom numbering. (b) The Ni_4O_3 core structure with the isosceles Ni_3 triangle base, highlighted in transparent blue, with μ_4-O sites of the lacunary cubane shown as red spheres. Butyl and isopropyl residues are not shown. Color code: Ni, green spheres; C, dark grey; N, blue; O, red. The terminal MeCN molecule is shown in ball-and-stick representation. Hydrogen atoms are omitted for clarity.

In 2007 Biswas et al.[14] reported an octadecanuclear $\{Ni_{16}Na_2\}$ coordination cluster composed of four $[Ni_4(Hmda)_3(OOCMe)_5$ $(OOCH)_{0.5}]$ fragments (H_2mda = N-methyldiethanolamine), interconnected via two sodium cations and two formate anions. The central Ni_4O_3 core (i.e. a lacunary Ni_4O_4 cubane core) in each of these fragments is isostructural to that in the isolated compound **2**. In 2005 Salameh et al.[15] prepared a cationic $[Ni_9L_8(OH)_6(NH_3)_4(H_2O)_8]^{4+}$ coordination cluster (HL = 7,8-dihydro-1,2,4-triazolo[4,3-α]pyrimidin-7-one), which comprises two $\{Ni_4\}$ fragments linked by six L ligands through a ninth Ni(ii) ion. In 1977 Strouse et al.[16] and in 2003 Murrie et al.[17] reported the compound $(NMe_4)_{10}[Ni_8(cit)_6(OH)_2(H_2O)_2]$ (H_4cit = citric acid), differing only in crystal packing and the number of lattice water molecules. This compound is a dimer of two $\{Ni_4\}$ fragments that are bridged by two μ_3-O atoms of two cit ligands. In addition, the Ni_4O_3 coordination has been observed in the chemistry of polyoxometalates,[18] where it was found to coordinate to polyoxotungstates to form $\{XW_9Ni_4\}$ building units, which are obtained by using e.g. nickel nitrate or nickel acetate and $Na_{10}[A-\alpha-XW_9O_{34}]\cdot nH_2O$ as precursors (X = Si, P). To the best of our knowledge, compound **2** represents the first example of a metal complex featuring a discrete, organic ligand-supported Ni_4O_3 core whose molecular ions are detectable in the ESI-MS spectrum in MeOH (see ESI†).

Another interesting feature of **2** is the weakly coordinated, labile MeCN molecule that can be regarded as a potential substrate docking position for catalytic conversions.[19] To probe the accessibility of this Ni4 site, we stirred compound **2** in MeOH at room temperature for several minutes. The microcrystalline product was filtered off and dried in air. EA indicates the composition $[Ni_4(Hbda)_3(ib)_5]\cdot MeOH\cdot 2H_2O$, thus suggesting that the MeCN molecule was readily replaced by MeOH or one of the two water solvent molecules (calcd/found: C, 44.34/44.28; H, 8.02/7.86 and N, 3.45/3.68%). Also, analysis of freshly prepared **2** that was washed with small amounts of MeCN and dried in air was performed several times. The results of these analyses show the following ranges: C, 43.2–43.7; H, 7.44–7.73; N, 2.93–2.98%. The low amount of C and N is indicative of de-coordination of the terminal MeCN molecule under the used mild conditions (air and moisture). Thus, the obtained C/H/N values indicate the formula $[Ni_4(Hbda)_3(ib)_5]\cdot 3H_2O$ [calcd: C, 43.86; H, 7.95; N, 3.49%]. This de-coordination is furthermore revealed by the absence of a CN band (ν(CN) of free MeCN: 2254 cm^{-1}) in the IR spectrum of compound **2**. The retention of the $\{Ni_4\}$ core is indicated by nearly identical IR fingerprints of compound **2** and its MeOH-treated derivative (Fig. S2 and S3†) as well as the obtained ESI-MS data (Fig. S7 and Table S3†).

Magnetism and magnetochemical modeling

For the analysis of the paramagnetic susceptibility caused by the three Co(ii) centers of compound **1**, we note that the octahedrally coordinated low-spin Co(iii) centers significantly contribute via their temperature-independent paramagnetism.[20] We assume $\chi_{TIP} = +0.4 \times 10^{-3}$ cm^3 mol^{-1} (ref. 20b) in total for both centers in **1**, thus obtaining $\chi_m T = 8.69$ cm^3 K mol^{-1} at 290 K instead of 8.80 cm^3 K mol^{-1}. The corresponding net data for three Co(ii) centers are shown in Fig. 3. The value of 8.69 cm^3 K mol^{-1} is in the range 6.94–9.78 cm^3 K

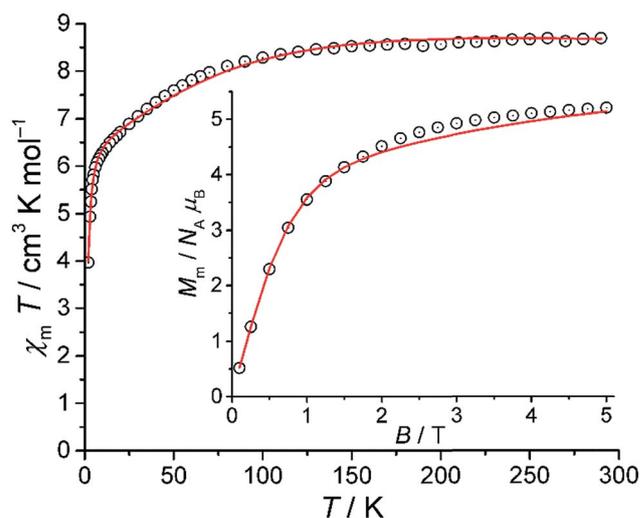**Fig. 3** Temperature dependence of $\chi_m T$ at 1.0 T of compound **1**; inset: molar magnetization M_m vs. B at 2.0 K: experimental data for three Co(ii) centers (open circles), least-squares fit (red solid lines).

mol^{-1} that is expected for three non-interacting high-spin Co(II) centers.[20a] With decreasing temperature, $\chi_m T$ is almost constant down to ca. 150 K, and subsequently decreases to 3.97 cm^3 K mol^{-1} at 2.0 K. The latter is caused by the split of the ^{4}F ground term of the free ion by the ligand field into a ^{4}T$_{1g}$ ground term (and excited ^{4}T$_{2g}$, ^{4}A$_{2g}$ terms) which is potentially further split due to the distorted octahedral geometry of the ligands.

Irrespective of a symmetry-decreasing distortion, spin–orbit coupling causes a split of the ^{4}T$_{1g}$ ground term in addition to mixing of excited states and ground state, which is reflected by a temperature dependence of $\chi_m T$ due to thermal (de)population of the resulting states. Additionally, antiferromagnetic exchange interactions may be present. The molar magnetization reaches 5.2 $N_A\mu_B$ at 5.0 T and 2.0 K, well below a saturation value of ca. 11–12 $N_A\mu_B$ extrapolated from the $\chi_m T$ value at ambient temperature. The magnetization does not, however, saturate as revealed by the small but distinct slope of M_m vs. B at this field. The magnetization behavior may be thus determined by antiferromagnetic exchange interactions and/or single-ion effects. Due to the structure of compound **1**, a chain of alternating Co(II) and Co(III) centers and extended –O–Co(III)–O– exchange pathways between the Co(II) centers, we expect negligible or very weak exchange interactions.

Using the "full model" Hamiltonian implemented in CONDON 2.0,[10] the magnetic data of compound **1** was modeled assuming the three Co(II) centers to be identical, and in a C_{4v}-symmetric ligand field. Potential exchange interactions are accounted for by a mean-field approach. Treating the standard Racah parameters $B = 1115$ cm^{-1} and $C = 4366$ cm^{-1} and the one-electron spin–orbit coupling parameter $\zeta_{3d} = 533$ cm^{-1} as constants,[21] we use the full basis of 120 states. The least-squares fit of goodness SQ = 1.6% yields the ligand field parameters $B_0^2 = (-5060 \pm 2130)$ cm^{-1}, $B_0^4 = (12\,247 \pm 2598)$ cm^{-1}, $B_4^4 = (29\,985 \pm 1088)$ cm^{-1} (in Wybourne notation) and $zJ' \leq -0.1$ cm^{-1} ($-2zJ'$ notation; Fig. 3). The mean-field parameter zJ' reveals very small antiferromagnetic exchange interactions. The ligand field parameters describe a ligand field of distorted octahedral symmetry which splits, along with the spin–orbit coupling, the ^{4}T$_{1g}$ ground term into six Kramers doublets. The first excited states are at ca. 190 cm^{-1}, 350 cm^{-1}, and 610 cm^{-1} above the ground state while the remaining two doublets are at ca. 3900 cm^{-1} and 4000 cm^{-1}.

The magnetic data of compound **2** are shown in Fig. 4 as $\chi_m T$ vs. T and M_m vs. B plots. At 290 K, the $\chi_m T$ value of 4.86 cm^3 K mol^{-1} lies within the range 3.92–6.13 cm^3 K mol^{-1} expected for four non-interacting high-spin Ni(II) centers.[20a] Upon temperature decrease, $\chi_m T$ slightly increases to a maximum of 4.93 cm^3 K mol^{-1} at 200 K, subsequently decreases to 4.45 cm^3 K mol^{-1} at 25 K, and falls off to a minimum of 3.64 cm^3 K mol^{-1} at 2.6 K. Since the ground term of octahedral Ni(II) centers is ^{3}A$_{2g}$, such compounds exhibit nearly spin-only paramagnetism, i.e. **2** may be described as system of effective spin-1 centers. The shape of the $\chi_m T$ vs. T curve is thus essentially due to weak exchange interactions of approximately same magnitude. The low-temperature data ($T < 30$ K) may, however, also be significantly influenced by effects of zero-field splitting which occurs for Ni(II) centers in case of ligand field symmetry distortion. Due
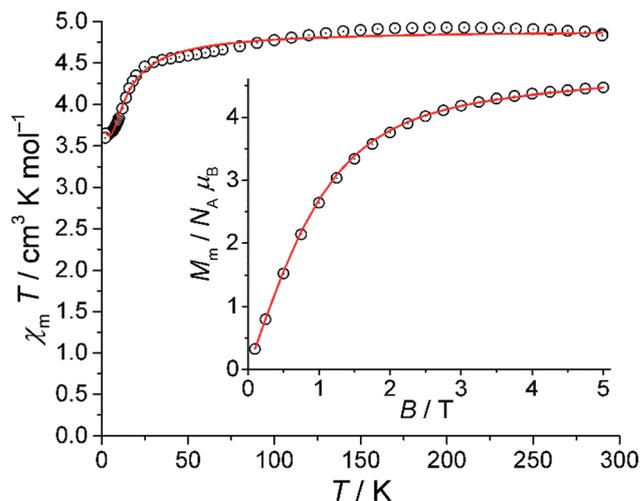

Fig. 4 Temperature dependence of $\chi_m T$ at 0.1 T of compound **2**; inset: molar magnetization M_m vs. B at 2.0 K: experimental data (open circles), least-squares fit (red solid lines).

to the spin-only nature of the Ni(II) centers, the magnetization curve at 2.0 K indicates a saturation step at about 4.5–5.0 $N_A\mu_B$, therefore indicating a total ground state $S = 2$ derived from $M_{m,step} = g_S S N_A\mu_B$, and $g_S > 2$ for Ni(II).

The magnetic data of compound **2** is reproduced by employing the spin-only option of CONDON 2.0.[10] Assuming approximately isotropic Ni(II) centers, we restrict the number of independent exchange interaction pathways to two to avoid over-parameterization. The parameters describing the interaction of the three Ni(II) centers forming an almost equilateral triangle of side length 3.8 Å are denoted as J_2, while the remaining three shorter pathways exhibiting Ni–Ni distances of ca. 3.0 Å are characterized by J_1. The least-squares fit of goodness SQ = 1.1% yields $J_1 = (-1.6 \pm 0.1)$ cm^{-1}, $J_2 = (+0.7 \pm 0.2)$ cm^{-1} and $g_{eff} = 2.21 \pm 0.02$ ($-2J$ notation). The corresponding calculated data are depicted as solid lines in Fig. 4. The calculated ground state is also characterized by $S = 2$. Introduction of additional exchange pathways does not significantly enhance the goodness-of-fit. The compound may thus be described as three centers with effective $S = 1$ forming a ferromagnetic coupled triangle that is opposed to a single spin-1 center which antiferromagnetically interacts with the triangle.

Conclusions

We showcased that the aerobic one-pot reaction of simple M(ib)$_2$ precursors (M = Co and Ni) with *N*-butyldiethanolamine results in starkly different polynuclear compounds with properties (charge neutrality, relatively high thermal stability, characteristic geometries) that render these species amenable for surface deposition: a mixed-valent Co(II/III) complex (**1**) with negligible antiferromagnetic interactions due to an alternating Co^{II}–Co^{III}–Co^{II}–Co^{III}–Co^{II} sequence, and a Ni(II) complex (**2**) with both ferromagnetic and antiferromagnetic nearest-neighbor coupling. The lacunary cubane structure of **2** was hitherto not known as discrete motif; **1** represents an entirely

different $Co^{II/III}$ valence pattern compared to the only other known $\{Co_5^{II/III}\}$ horseshoe cluster.[13] The ligand environments at certain metal sites are in principle conducive to facile metathesis, an important aspect for a potential catalytic functionality that we plan to explore in the future.

Experimental

Materials and methods

Compounds **1** and **2** were synthesized under aerobic conditions. All starting materials were from commercial sources and used as received. Solvents were used without further purification. The IR spectra of compounds **1** and **2** were recorded on a Nicolet Avatar 360 FTIR spectrometer (KBr pellets, $\nu = 4000\text{--}400\ cm^{-1}$). TG/DT analyses of compounds **1** and **2** were performed under N_2 flow and a heating rate of $5\ K\ min^{-1}$ in the temperature range 25–800 °C on a Mettler Toledo TGA/SDTA 851e instrument. The ESI-MS spectra of compounds **1** and **2** in the positive ion mode was recorded on a 4000 QTRAP mass spectrometer system, using the LC/LC-MS method with direct infusion.

Synthesis of $[Co_3^{II}Co_2^{III}(Hbda)_2(bda)_2(ib)_6]\cdot 2MeCN$ (1)

A 10 mL MeCN solution of freshly prepared $Co(ib)_2$ (0.233 g; 1.0 mmol) and *N*-butyldiethanolamine (0.170 mL; 1.0 mmol) were stirred under reflux for 1 h to give a clear violet solution. The MeCN solution was filtered off and the filtrate was kept in a capped vial at room temperature. The color of solution became dark green with time. After two days the dark-green block-shaped single crystals suitable for single-crystal X-ray diffraction analysis were obtained. Yield: 0.143 g (49% based on Co). Elemental analysis, calcd for $C_{56}Co_5H_{112}N_4O_{20}$ (1456.17 g mol^{-1}; no solvent): Co, 20.24; C, 46.19; H, 7.75; N, 3.85%. Found: Co, 20.6; C, 46.13; H, 7.80; N, 3.63%. IR (KBr pellet), ν_{max}/cm^{-1}: 3434 (m, br), 2960 (s), 2930 (sh), 2868 (sh), 1614 (s), 1577 (vs), 1537 (sh), 1469 (s), 1414 (s), 1371 (m), 1357 (sh), 1296 (m), 1169 (w), 1092 (s), 1029 (sh), 1015 (sh), 984 (w), 917 (m), 827 (w), 767 (w), 641 (w), 584 (w), 546 (w), 522 (w), 496 (w). MS (MeOH, ESI): m/z: 1280.355 ($C_{48}Co_5H_{97}N_4O_{16}^+$, 100%; $[Co_5(Hbda)_1(bda)_3(ib)_4]^+$–ib–Hib); 1368.407 ($C_{52}Co_5H_{105}N_4O_{18}^+$, 82%; $[Co_5(Hbda)_2(bda)_2(ib)_5]^+$–ib); 1192.303 ($C_{44}Co_5H_{89}N_4O_{14}^+$, 27%; $[Co_5(bda)_4(ib)_3]^+$–ib–2Hib); 757.193 ($C_{28}Co_3H_{56}N_2O_{10}^+$, 23%; $[Co_3(Hbda)_2(ib)_3]^+$–3ib–2bda).

Synthesis of $[Ni_4(Hbda)_3(ib)_5(MeCN)]$ (2)

A 10 mL MeCN of freshly prepared $Ni(ib)_2$ (0.233 g; 1.0 mmol) and *N*-butyldiethanolamine (0.170 mL; 1.0 mmol) were stirred under reflux for 1 h to give a clear green solution. The MeCN solution was filtered off and the filtrate was kept in a capped vial at room temperature. The light-green block-shaped single crystals suitable for single-crystal X-ray diffraction analysis were obtained after one week. Yield: 0.065 g (22% based on Ni). Elemental analysis, calcd for $C_{46}H_{92}N_4Ni_4O_{16}$ (1192.01 g mol^{-1}; no solvent): see discussion above. IR (KBr pellet), ν_{max}/cm^{-1}: 3423 (s, br), 2964 (s), 2930 (sh), 2876 (sh), 1620 (s), 1587 (sh), 1557 (vs), 1474 (s), 1427 (s), 1373 (m), 1360 (sh), 1287 (m), 1169 (w), 1142 (w), 1095 (w), 1067 (m), 1026 (sh), 980 (w), 905 (m), 891

(sh), 859 (w), 832 (m), 779 (w), 675 (w), 616 (w), 580 (w), 448 (w). MS (MeOH, ESI): m/z: 1006.201 ($C_{37}H_{78}N_3Ni_4O_{13}^+$, 100%; $[Ni_4(Hbda)_2(bda)_1(ib)_3(MeOH)]^+$–ib–Hib–MeCN + MeOH); 974.265 ($C_{36}H_{74}N_3Ni_4O_{12}^+$, 72%; $[Ni_4(Hbda)_2(bda)_1(ib)_3]^+$–MeOH); 886.212 ($C_{32}H_{66}N_3Ni_4O_{10}^+$, 38%; $[Ni_4(Hbda)_1(bda)_2(ib)_2]^+$–Hib); 798.160 ($C_{28}H_{58}N_3Ni_4O_8^+$, 28%; $[Ni_4(bda)_3(ib)_1]^+$–Hib).

X-ray crystallography

Single-crystal diffraction data for compounds **1** and **2** were collected on an Agilent Technologies SuperNova diffractometer with MoKα radiation ($\lambda = 0.71073$ Å) at 120 K. The crystals were mounted in a Hampton cryoloop with Paratone-N oil to prevent solvent loss. Absorption corrections were applied numerically based on multifaceted crystal model using CrysAlis software.[22] The SHELXTL software package[23] was used to solve and refine the structure. The structures were solved by direct methods and refined by full-matrix least-squares method against $|F|^2$ with anisotropic thermal parameters for all atoms besides hydrogens. The hydrogen atoms of the OH groups of $Hbda^-$ and bda^{2-} ligands as well as CH_3 groups of co-crystallized solvent molecules in compound **1** were not located. Also in the both structures (**1** and **2**) disorder of the butyl moiety of one of the (H)bda^- and $CH(CH_3)_2$ groups of several ib^- ligands precluded a possibility for calculation of some geometrical positions of hydrogen atoms, therefore we decided to not include these hydrogens in the model for **1** and any hydrogens into the model for **2** (the final formulae in the CIFs for the both compounds contain all hydrogen atoms for overall consistency). The relative site occupancy factors for the disordered positions of carbon atoms were refined using combination of PART and EADP instructions. DELU restrictions had to be applied to some carbon atoms of the disordered $Hbda^-$ ligands in compound **2**. Additional crystallographic data are summarized Table S1 in the ESI.†

Magnetic susceptibility measurements

Magnetic susceptibility data of compounds **1** and **2** were recorded using a Quantum Design MPMS-5XL SQUID magnetometer. The polycrystalline samples were immobilized into PTFE capsules. The data were acquired as a function of the field (0.1–5.0 T) and temperature (2.0–290.0 K) and were corrected for diamagnetic contributions from the sample holder and the compounds ($\chi_{dia} = -7.28 \times 10^{-4}\ cm^3\ mol^{-1}$ (**1**), $-5.96 \times 10^{-4}\ cm^3\ mol^{-1}$ (**2**)).

Notes and references

1 (*a*) S. Goswami, A. K. Mondal and S. Konar, *Inorg. Chem. Front.*, 2015, **2**, 687; (*b*) Y.-Z. Zheng, Z. Zheng and

X.-M. Chen, *Coord. Chem. Rev.*, 2014, **258–259**, 1; (*c*) A. Palii, B. Tsukerblat, S. Klokishner, K. R. Dunbar, J. M. Clemente-Juan and E. Coronado, *Chem. Soc. Rev.*, 2011, **40**, 3130; (*d*) D.-F. Weng, Z.-M. Wang and S. Gao, *Chem. Soc. Rev.*, 2011, **40**, 3157; (*e*) M. Murrie, *Chem. Soc. Rev.*, 2010, **39**, 1986; (*f*) P. Chaudhuri, *Coord. Chem. Rev.*, 2003, **243**, 143.

2 (*a*) L. Bogani and W. Wernsdorfer, *Nat. Mater.*, 2008, **7**, 179; (*b*) S. Sanvito, *Chem. Soc. Rev.*, 2011, **40**, 3336; (*c*) D. E. Bürgler, V. Heß, T. Esat, S. Fahrendorf, F. Matthes, C. M. Schneider, C. Besson, K. Y. Monakhov, P. Kögerler, A. Ghisolfi, P. Braunstein, N. Atodiresei, V. Caciuc and S. Blügel, *e-J. Surf. Sci. Nanotechnol.*, 2016, **14**, 17.

3 See the RSC themed collection on "Molecular spintronics and quantum computing": E. Coronado and A. J. Epstein, *J. Mater. Chem.*, 2009, **19**, 1670.

4 See the ACS virtual issue on "Quantum Molecular Magnets": K. R. Dunbar, *Inorg. Chem.*, 2012, **51**, 12055.

5 (*a*) A. Cornia, M. Mannini, P. Sainctavit and R. Sessoli, *Chem. Soc. Rev.*, 2011, **40**, 3076; (*b*) J. A. J. Burgess, L. Malavolti, V. Lanzilotto, M. Mannini, S. Yan, S. Ninova, F. Totti, S. Rolf-Pissarczyk, A. Cornia, R. Sessoli and S. Loth, *Nat. Commun.*, 2015, **6**, 8216.

6 J. Dreiser, A. M. Ako, C. Wäckerlin, J. Heidler, C. E. Anson, A. K. Powell, C. Piamonteze, F. Nolting, S. Rusponi and H. Brune, *J. Phys. Chem. C*, 2015, **119**, 3550.

7 (*a*) F. K. Larsen, J. Overgaard, S. Parsons, E. Rentschler, A. A. Smith, G. A. Timco and R. E. P. Winpenny, *Angew. Chem., Int. Ed.*, 2003, **42**, 5978; (*b*) M. Rancan, G. N. Newton, C. A. Muryn, R. G. Pritchard, G. A. Timco, L. Cronin and R. E. P. Winpenny, *Chem. Commun.*, 2008, 1560; (*c*) A. McRobbie, A. R. Sarwar, S. Yeninas, H. Nowell, M. L. Baker, D. Allan, M. Luban, C. A. Muryn, R. G. Pritchard, R. Prozorov, G. A. Timco, F. Tuna, G. F. S. Whitehead and R. E. P. Winpenny, *Chem. Commun.*, 2011, **47**, 6251; (*d*) S. Schmitz, J. van Leusen, A. Ellern, P. Kögerler and K. Y. Monakhov, *Inorg. Chem. Front.*, 2016, **3**, 523.

8 See, *e.g.*: (*a*) S. Hameury, L. Kayser, R. Pattacini, G. Rogez, W. Wernsdorfer and P. Braunstein, *Dalton Trans.*, 2013, **42**, 5013; (*b*) N. Marino, D. Armentano, T. F. Mastropietro, M. Julve, G. De Munno and J. Martínez-Lillo, *Inorg. Chem.*,

2013, **52**, 11934; (*c*) F. J. Klinke, A. Das, S. Demeshko, S. Dechert and F. Meyer, *Inorg. Chem.*, 2014, **53**, 2976.

9 See, *e.g.*: (*a*) S. Schmitz, J. van Leusen, A. Ellern, P. Kögerler and K. Y. Monakhov, *Inorg. Chem. Front.*, 2015, **2**, 1095; (*b*) A. Ghisolfi, K. Y. Monakhov, R. Pattacini, P. Braunstein, X. López, C. de Graaf, M. Speldrich, J. van Leusen, H. Schilder and P. Kögerler, *Dalton Trans.*, 2014, **43**, 7847.

10 J. van Leusen, M. Speldrich, H. Schilder and P. Kögerler, *Coord. Chem. Rev.*, 2015, **289–290**, 137.

11 I. L. Malaestean, M. Speldrich, A. Ellern, S. G. Baca and P. Kögerler, *Polyhedron*, 2010, **29**, 1990.

12 I. L. Malaestean, S. Schmitz, A. Ellern and P. Kögerler, *Acta Crystallogr., Sect. C: Cryst. Struct. Commun.*, 2013, **69**, 1144.

13 I. C. Lazzarini, A. V. Funes, L. Carrella, L. Sorace, E. Rentschler and P. Alborés, *Eur. J. Inorg. Chem.*, 2014, 2561.

14 B. Biswas, S. Khanra, T. Weyhermüller and P. Chaudhuri, *Chem. Commun.*, 2007, 1059.

15 S. Salameh, M. Abul-Haj, M. Quirós and J. M. Salas, *Eur. J. Inorg. Chem.*, 2005, 2779.

16 J. Strouse, S. W. Layten and C. E. Strouse, *J. Am. Chem. Soc.*, 1977, **99**, 562.

17 M. Murrie, D. Biner, H. Stoeckli-Evans and H. U. Güdel, *Chem. Commun.*, 2003, 230.

18 (*a*) U. Kortz, A. Tézé and G. Hervé, *Inorg. Chem.*, 1999, **38**, 2038; (*b*) C. Pichon, P. Mialane, A. Dolbecq, J. Marrot, E. Rivière, B. S. Bassil, U. Kortz, B. Keita, L. Nadjo and F. Sècheresse, *Inorg. Chem.*, 2008, **47**, 11120; (*c*) G. Rousseau, E. Rivière, A. Dolbecq, J. Marrot, O. Oms and P. Mialane, *Eur. J. Inorg. Chem.*, 2013, 1793; (*d*) G. Rousseau, O. Oms, A. Dolbecq, J. Marrot and P. Mialane, *Inorg. Chem.*, 2011, **50**, 7376.

19 P. Zhang, M. Wang, Y. Yang, D. Zheng, K. Han and L. Sun, *Chem. Commun.*, 2014, **50**, 14153.

20 (*a*) H. Lueken, *Magnetochemie*, Teubner Verlag, Stuttgart, 1999; (*b*) P. Cossee, *J. Inorg. Nucl. Chem.*, 1958, **8**, 483.

21 J. S. Griffith, *The Theory of Transition-Metal Ions*, Cambridge University Press, Cambridge, 2009.

22 CrysAlisPro, *Agilent Technologies, 1.171.36.28*, release 01-02-2013, CrysAlis171.NET.

23 G. M. Sheldrick, *Acta Crystallogr., Sect. A: Found. Crystallogr.*, 2008, **64**, 112.